

# Relativistic BWO with Mechanical Frequency Tuning<sup>1</sup>

E.M. Totmeninov, S.D. Korovin, A.I. Klimov, V.V. Rostov

*Institute of High Current Electronics SB RAS, 2/3 Akademicheskoy Ave., Tomsk, 634055, Russia  
ph. +7(3822)491-641, fax +7(3822)492-410, e-mail totm@lfe.hcei.tsc.ru*

**Abstract** – The paper presents experimental studies of broadband frequency tuning in the relativistic backward-wave oscillator (BWO) with increased cross-section of the electrodynamic system and a resonant wave reflector. The tuning within 12% band was realized by mechanically shifting the reflector about the slow-wave structure (SWS). No variation of the driving electron beam was used. With magnetic field of 4.6 kOe, the maximum microwave power in the limits of the tuning band was  $4 \pm 1$  GW at 3.6 GHz.

## 1. Introduction

Recently, considerable attention has been paid to development of relativistic HPM sources with the capability of broadband frequency tuning. In particular, the issue of tunability was studied for the relativistic backward-wave oscillator (BWO), which is known to be as an efficient HPM source in the X- and S-bands. The device possesses fast buildup of oscillation and is well adaptive to driving electron beam parameters. One of the ways to change the BWO generation frequency is variation of the electron energy; however, in the substantially relativistic range of energies this mechanism is not effective. At the same time, the BWO frequency may be tuned without variation of electron beam parameters. In the conventional BWO, moving the beyond cutoff-neck about the SWS was shown to change the frequency for 3–4% [1]. Further, in the resonant BWO [2], variation the SWS corrugation period with consistent correction of the tube full length allowed broadening of the frequency tuning range to about 15%. Both devices [1, 2] efficiently worked with strong guide magnetic fields (above the cyclotron resonance).

In the BWO with resonant reflector, which was reported earlier in [3] and is considered in this paper, it is possible to change the generation frequency without variation of the SWS period. This capability is due to the effect of preliminary modulation of beam electrons by energy occurring in the region of the resonant reflector. The energy modulation causes modulation of electron velocity and their inertial bunching. Changing the drift distance between the reflector and the corrugated slow-wave structure allows variation of the phase of the beam RF current with respect to RF field of the synchronous harmonic at the SWS input (below referred to as the modulation phase). The value of this

phase affects the device starting length and, which is essential, the starting synchronism mismatch and frequency. It is important that the corresponding range of frequency variation broadens with electron energy modulation depth in the reflector area.

This paper presents the studies of frequency tuning in an S-band BWO of this type.

The increased cross size of the electrodynamic system not only decreases the probability of its RF breakdown but also creates the necessary prerequisites for efficient operation of the device in the low magnetic field range [4] (below the cyclotron resonance).

## 2. Theoretical Background and Simulations

The relativistic BWO with increased SWS cross-section ( $D/\lambda > 1$ , with  $D$  being the mean diameter of the SWS and  $\lambda$  being the wavelength) is schematically depicted in Fig. 1.

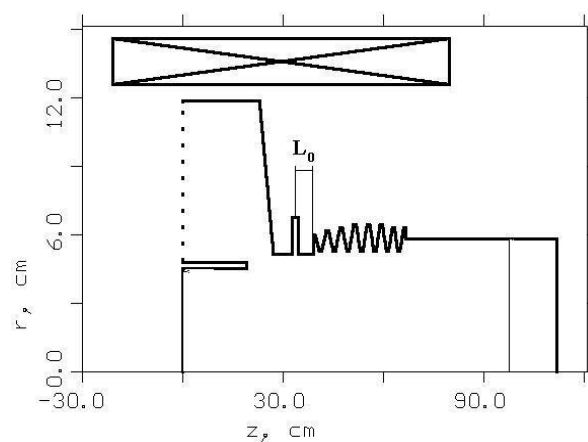


Fig. 1. BWO with resonant reflector

The backward  $TM_{01}$  wave is reflected from the resonant reflector at the cathode edge of the device due to excitation of locked  $TM_{02}$  oscillation in the reflector [3].

### A. Hydrodynamic model of BWO with electron beam premodulation (ultrarelativistic approximation)

In the ultra-relativistic limit ( $\gamma \gg 1$ ) the equation set describing the electron motion and the backward electromagnetic wave is written as:

$$\frac{dW}{d\zeta} = \text{Re}(F + i\sigma_0 J)e^{i\theta};$$

<sup>1</sup> Work has been supported by the Commissariat à l'Énergie Atomique, France.

$$\frac{d\theta}{d\zeta} = W^{-2} - \delta; \quad (1)$$

$$\frac{dF}{d\zeta} = IJ, \quad J = \int_0^{2\pi} e^{-i\theta} d\theta_0,$$

here  $\theta = \theta(\zeta, \theta_0)$  is the phase of synchronous wave acting on electron,  $\theta_0$  is the phase at the point of injection ( $\zeta = 0$ ),  $F = 2\gamma_0 e E_{-1}(r_b, z)/(kmc^2)$  is the dimensionless amplitude of electric field  $z$  – component at the beam radius ( $r_b$ ),  $W = \gamma/\gamma_0$ ,  $\zeta = kz/(2\gamma_0^2)$  is the dimensionless longitudinal coordinate,  $\delta = 2\gamma_0^2(h_{-1}/k - 1)$  – synchronism mismatch,  $I = 2\gamma_0^3 e Z_{-1} I_b / (\pi mc^2)$  – normalized parameter of current,  $Z_{-1}$  – coupling impedance for the synchronous harmonic,  $\sigma_0$  – parameter of space charge,  $K = 2\pi/\lambda$ ,  $\lambda$  – radiation wavelength,  $\gamma_0$  – initial relativistic factor of electrons.

With  $L_0 \ll L_k$ , where  $L_0$  is the length of the drift space and  $L_k$  is the generator full length, the boundary conditions for the set (1) are as follows:

$$\begin{aligned} W(\zeta_0, \theta_0) &= 1 + \operatorname{Re}(\alpha F(\zeta_0) e^{i\theta_0}), \\ \theta(\zeta_0, \theta_0) &= \theta_0 + (W^{-2}(\zeta_0, \theta_0) - \delta)\zeta_0, \\ F(\zeta_k) &= 0, \end{aligned} \quad (2)$$

where  $\zeta_k = kL_k/2\gamma_0^2$ ,  $\zeta_0 = kL_0/2\gamma_0^2$ ,  $\theta_0 \in [0, 2\pi)$ ,  $\alpha$  is the complex parameter of modulation [3].

The value  $|\alpha|$  determines the electron velocity modulation depth in the reflector area.

The value  $\arg(\alpha)$  – the modulation phase – defines the position of the electron bunch in the synchronous wave at the entrance of the SWS. If  $\zeta_0 \ll 1$ , then  $\arg(\alpha)$  is determined by the reflector position relative to the SWS ( $L_0$ ) and may be considered to be an independent parameter.

The efficiency of energy exchange between electrons and the RF field is defined as

$$\eta = \frac{\gamma_0}{\gamma_0 - 1} \left( 1 - \frac{1}{2\pi} \int_0^{2\pi} W(\zeta_k, \theta_0) d\theta_0 \right) = \frac{\gamma_0}{\gamma_0 - 1} \hat{\eta}, \quad (3)$$

here  $\hat{\eta}$  is the normalized efficiency.

Results of linear (starting-regime) solution of eqs. (1), (2) with small space charge parameter ( $\sigma_0 \ll 1$ ) are illustrated in Fig. 2.

With a fixed length of the SWS, the starting current reduces with the modulation depth over a wide range of  $\arg(\alpha)$  (Fig. 2a).

Another peculiarity of the generator starting conditions is that the synchronism mismatch ( $\delta$ ) depends on  $\arg(\alpha)$  and this dependence becomes stronger with modulation depth (Fig. 2b). Thus, preliminary modulation enables variation of the generation frequency. Fig. 3 presents typical nonlinear solutions of the problem (1), (2) obtained with small space charge field.

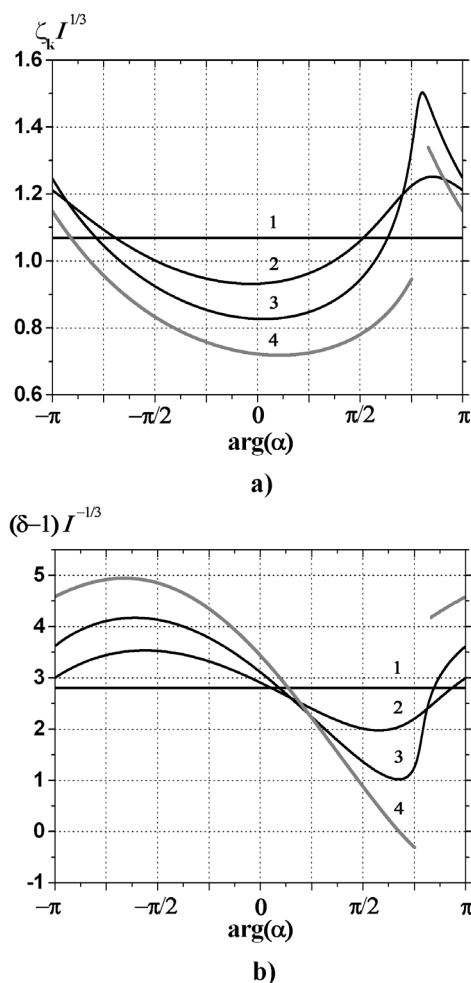


Fig. 2. Starting eigenvalues for the first longitudinal mode vs modulation phase, with different values of  $|\alpha| (I)^{1/3}$ : 1 – 0; 2 – 0.15; 3 – 0.3; 4 – 0.5

With optimum position of the reflector, the microwave power efficiency of the generator in the ultra-relativistic case can reach 40%. It is important that the dependence of synchronism mismatch on the reflector position remains the same in non-linear regime.

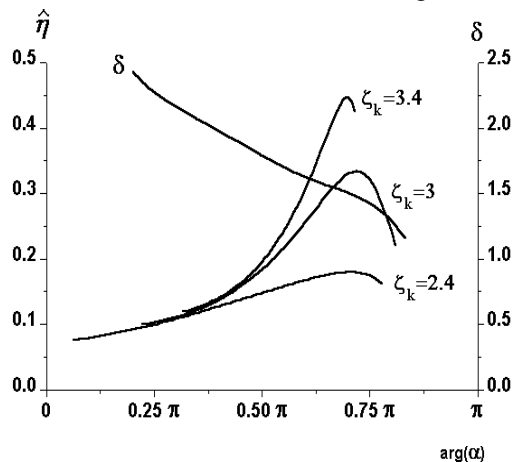


Fig. 3. Dependencies of normalized efficiency and synchronism mismatch on the modulation phase for various SWS lengths ( $I = 0.1$ ,  $|\alpha| = 1.1$ ,  $\sigma_0 \ll 1$ ,  $\zeta_0 \ll 1$ )

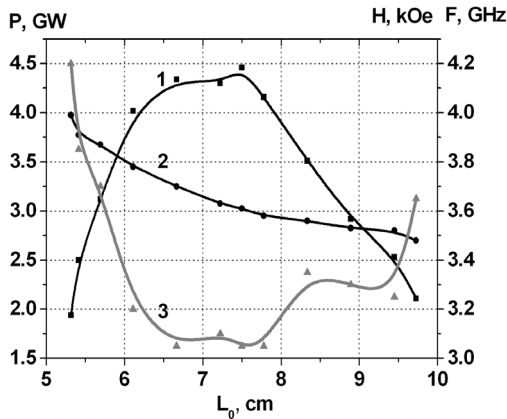


Fig. 4. Simulated dependences of (1) microwave power (steady-state regime), (2) frequency, and (3) optimum magnetic field strength on the drift space length  $L_0$

If the condition of  $\zeta_0 \ll 1$  is not satisfied, then the problem requires self-consistent solution. In this case,  $\arg(\alpha)$  is not independent and must be found from the equation system (1), (2). Numerical simulation indicated that in this case there is also dependence of synchronism mismatch on the reflector position.

### B. Simulation

Optimization of the generator in simulation was made using the KARAT code [5]. The simulated area is depicted in Fig. 1. The mean diameter of the SWS was about  $1.5 \lambda$ . The optimum parameters of electron beam found in simulation were: diode voltage 1.2 MV, electron beam current 12.5 kA. The operation mode was  $TM_{01}$ . Stable generation was observed in the range of magnetic fields from 2.5 up to 4.5 kOe. Below this interval, the generation efficiency was limited by intense pumping of transverse velocities of electrons in the region of the vacuum diode, and above this interval – by the cyclotron absorption of the backward wave.

The frequency shift obtained in simulation was  $dF/dL_0 \approx 100$  MHz/cm (Fig. 4).

Near the limits of the frequency tuning band, larger oscillation buildup time was observed in simulation. This is possibly because, in the limit positions of the reflector, the starting current approaches and even exceeds the value corresponding to no modulation (Fig. 2a). In the simulation, obtaining the maximum tuning bandwidth of  $\sim 14\%$  at half power level (3.48–3.95 GHz) required slight adjustment of the guide magnetic field strength. This was apparently because the change in frequency caused some changed in the conditions for cyclotron absorption of the backward wave. The maximum simulated power was  $\sim 4.5$  GW with 32% power efficiency.

### 3. Experiment

Experiments were performed with the SINUS-7 [6] electron accelerator (50 ns pulse width) in single-pulse regime. The diode voltage was  $\sim 1.2$  MV and the total

diode current was  $\sim 16$  kA. The amplitude of electron current injected in the BWO slow-wave structure increased with magnetic field and stabilized at 13 kA with  $H \approx 4.0$  kOe as the electron beam fully passed in the waveguide adjacent to the resonant reflector. The substantial ( $\sim 3$  kA) difference between the full current and the injected current was apparently because of current leakage in the diode (parasitic explosive emission from metal surface of the cathode-holder).

The microwave power was measured using an undirected strip-line coupler built in the output waveguide of the BWO, a short symmetric dipole receiving antenna, and an aperture type calorimeter (a planar calorimeter situated in air just behind the vacuum window). The microwave signal was detected with a coaxial semiconductor detector. The oscillation spectrum was measured using a heterodyne mixer.

Typical waveforms of the diode voltage, diode current, detected signal from microwave coupler, and the oscillation spectrum are presented in Fig. 5.

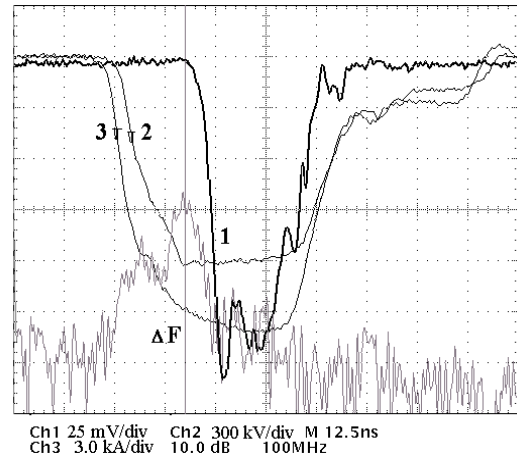


Fig. 5. 1 – microwave signal, 2 – diode voltage, 3 – diode current,  $\Delta F$  – shifted microwave spectrum ( $H \approx 4.6$  kOe,  $F_{\text{het}} = 3.9$  GHz,  $F_{\text{gen}} \approx 3.6$  GHz)

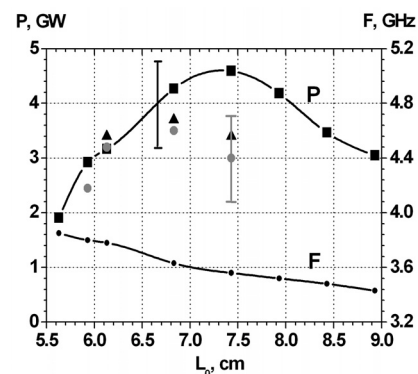


Fig. 6. Microwave peak power and frequency vs. position of the reflector (squares – peak power measured using the coupler, triangles – using aperture type calorimeter, circles – using the dipole antenna)

The corresponding position of the resonant reflector is  $L_0 = 7.4$  cm. The maximum microwave power was

$4 \pm 1$  GW, with 25% efficiency at 3.6 GHz. The radiation pattern corresponded to the  $TM_{01}$  wave.

Some irregularity of the microwave signal shape is apparently due to partial reflection of the wave from the output window.

The curve of frequency tuning obtained in the experiment is depicted in Fig. 6. For each value of  $L_0$ , slight adjustment of magnetic field was made (in the limits of 4.1–4.9 kOe).

Unlike numerical simulation, the microwave pulse amplitude, width and frequency were unstable near the boundaries of the tuning band. This was apparently due to concurrence by parasitic oscillation at 3.2 GHz and 4.5 GHz and incomplete development of generation because of the increased rise time.

## References

- [1] S.D. Korovin, S.D. Polevin, A.M. Roitman et al., *Izvestiya vuzov. Fizika* **39**, 12, 49 (1996).
- [2] S.A. Kitsanov, A.I. Klimov, S.D. Korovin et al., *Pis'ma v ZhTF* **29**, 6, 87 (2003).
- [3] S.D. Korovin, I.K. Kurkan, V.V. Rostov et al., *Izvestiya vuzov. Radiofizika* **42**, 12, 1189 (1999).
- [4] I.K. Kurkan, V.V. Rostov, E.M. Totmeninov, *Pis'ma v ZhTF* **24**, 10, 43 (1998).
- [5] V.P. Tarakanov. *User's Manual for Code KARAT*. Springfield, VA: BRA, 1992.
- [6] G.A. Mesyats, S.D. Korovin, A.V. Gunin et al., *Laser and Particle Beams* **21**, 2, 197 (2003).